ISSN 1674-1056
http://cpb.iphy.ac.cn
http://iopscience.iop.org/cpb
中国物理 B
Chinese Physics
中国物理 Chinese Physics B

Electron-impact single ionizaiton for W^{4+} and W^{5+}

Denghong Zhang(张登红), Luyou Xie(颉录有), Jun Jiang(蒋军), Zhongwen Wu(武中文), Chenzhong Dong(董晨钟), Yinglong Shi(师应龙), Yizhi Qu(屈一至)
Citation: Chin. Phys. B . 2018, 27(5): 053402. **doi:** 10.1088/1674-1056/27/5/053402

Journal homepage: http://cpb.iphy.ac.cn; http://iopscience.iop.org/cpb

What follows is a list of articles you may be interested in

Differential cross sections of positron—hydrogen collisions

Rong-Mei Yu(于荣梅), Chun-Ying Pu(濮春英), Xiao-Yu Huang(黄晓玉), Fu-Rong Yin(殷复荣), Xu-Yan Liu(刘旭焱), Li-Guang Jiao(焦利光), Ya-Jun Zhou(周雅君)
Chin. Phys. B . 2016, 25(7): 073401. **doi:** 10.1088/1674-1056/25/7/073401

Differential cross sections for electron impact excitation of molecular hydrogen using the momentum-space multichannel optical method

Yuan-Cheng Wang(王远成), Jia Ma(马佳), Ya-Jun Zhou(周雅君)
Chin. Phys. B . 2016, 25(4): 043401. **doi:** 10.1088/1674-1056/25/4/043401

Production of projectile and target *K*-vacancy in near-symmetric collisions of 60-100 MeV Cu^{9+} ions with thin Zn target

Yipan Guo(郭义盼), Zhihu Yang(杨治虎), Shubin Du(杜树斌), Hongwei Chang(常宏伟), Qingliang Xia(夏清良), Qiumei Xu(徐秋梅)
Chin. Phys. B . 2016, 25(3): 033401. **doi:** 10.1088/1674-1056/25/3/033401

Energy and rotation-dependent stereodynamics of $H(^2S) + NH(a^1\Delta) \rightarrow H_2(X^1\Sigma_g^+) + N(^2D)$ reaction

Yong-Qing Li(李永庆), Yun-Fan Yang(杨云帆), Yang Yu(于洋), Yong-jia Zhang(张永嘉), Feng-Cai Ma(马凤才)
Chin. Phys. B . 2016, 25(2): 023401. **doi:** 10.1088/1674-1056/25/2/023401

Triple differential cross sections of magnesium in doubly symmetric geometry

S Y Sun(孙世艳), X Y Miao(苗向阳), Xiang-Fu Jia(贾祥富)
Chin. Phys. B . 2016, 25(1): 013401. **doi:** 10.1088/1674-1056/25/1/013401

Electron-impact single ionizaiton for W^{4+} and W^{5+}*

Denghong Zhang(张登红)[1,†], Luyou Xie(颉录有)[1], Jun Jiang(蒋军)[1], Zhongwen Wu(武中文)[1], Chenzhong Dong(董晨钟)[1], Yinglong Shi(师应龙)[2], and Yizhi Qu(屈一至)[3]

[1] *Key Laboratory of Atomic and Molecular Physics & Functional Materials of Gansu Province, College of Physics and Electronic Engineering, Northwest Normal University, Lanzhou* 730070, *China*

[2] *Department of physics, Tianshui Normal University, Tianshui* 741000, *China*

[3] *College of Material Sciences and Opto-electronic Technology, University of Chinese Academy of Sciences, Beijing* 100049, *China*

(Received 22 January 2018; revised manuscript received 6 March 2018; published online 26 April 2018)

Electron-impact single ionization cross sections for W^{q+} ($q = 4$–5) were calculated using the flexible atomic code (FAC) in the level-to-level distorted-wave method, considering the explicit branching ratio. The calculated cross sections are compared with the available theoretical and experiment results in detail. In the case of the contribution from the same channles as the available theoretical results, all of the calculated ionization cross sections agree with the experimental measured cross sections. But the present calculated results are larger than the experimental measurement when all channels contributions are included. Some important channels excitation autoionization (EA) contributions, such as the excitation to higher higher nl' subshell from 4f and 5[s,p], were not included into the available theoretical calculation. In general, the distorted-wave (DW) results are overestimated.

Keywords: tungsten ions, electron-impact ionization, cross section

PACS: 34.50.Fa, 34.80.Dp, 32.80.Aa **DOI:** 10.1088/1674-1056/27/5/053402

1. Introduction

Tungsten (W) has the highest melting point of pure metal and also has low tritium retention, which make it ideal for the environment of a tokamak. Tungsten is currently a promising plasma-facing material in a fusion reactor.[1] In early tokamaks, such as the Symmetric Torus (ST) at Princeton[2] and the Oak Ridge Tokamak (ORMAK) in Tennessee,[3] tungsten was often used as a limiter. At that time, tungsten was expected to not be used in high-power machines, because its strong radiation losses would likely quench the ignition of a deuterium–tritium plasma.[4] But late experimental results at the Asymmetric Divertor Experiment (ASDEX) Upgrade and the Joint European Torus (JET) showed that W could be used in tokamaks without disrupting the fusion process.[5] Now W is to be used as the plasma-facing material not only for the baffles but also for the target plates of the International Thermonuclear Experimental Reactor (ITER),[6] which has renewed interest in the properties of tungsten as a plasma-facing material. Tungsten is now one of the most studied elements.[5] As heavy impurity ions, tungsten unavoidable migrates to the core plasma by physical sputtering. Therefore, detailed knowledge about atomic processes and about the atomic structure of tungsten in all charged states is definitely required to properly understand the influence of tungsten as a plasma impurity on the plasma performance.[7]

Electron-impact ionization (EII) is an essential collisional atomic process in fusion plasma and the reliable data are necessary for the spectroscopic modeling and analysis.[8] In past years, there have been some investigations associated with EII of tungsten. In experimental aspects, single and multiple EII of W^{q+} ions in charged states $q = 1$–10 were measured employing the cross-beams technique a couple of decades ago.[9–11] Single and double EII cross sections for W^{17+} have only recently been measured using an electron–ion crossed-beam setup by Rausch *et al.*[12] Very recently, Spruck *et al.* again measured the absolute cross section for EII of W^{q+} ($q \leq 17$) ions.[13] In theoretical aspects, the calculations for the EII cross section of tungsten ions are challenging due to its pronounced many-electron, relativistic effects, and the presence of open d or f shells. Therefore, some semi-empirical methods, such as the widely used Lotz expression,[10] binary-encounter Bethe (BEB) model,[14,15] and configuration-averaged distorted-wave (CADW) method,[16–19] were often used for prediction. For example, Kwon *et al.* reported calculated EII cross sections of the neutral W atom and W^+ ion using the BEB model.[14] Electron-impact single ionization (EISI) for the ground state of all charged states W ions were investigated using the CADW method[16–19] and the Maxwellian rate coefficients for plasma modeling have been provided in a website of the Oak Ridge National Laboratory (ORNL) Controlled Fusion Atomic Data Center (CFADC).[19] Vainshtein *et al.* calculated EII cross sections and rate coefficients of the atom W and W^+ using the Coulomb–Born method with exchange and

*Project supported by the National Natural Science Foundation of China (Grant Nos. 2017YFA0402300, 11464042, 11564036, 11774292, and 11464040) and the Basic Scientific Research Foundation for Institution of Higher Learning of Gansu Province, China.

†Corresponding author. E-mail: zhangdh@nwnu.edu.cn

© 2018 Chinese Physical Society and IOP Publishing Ltd

normalization.[20] Ballance *et al.* calculated direct ionization (DI) using the level-to-level distorted-wave (LLDW) approximation and the contributions of excitation autoionization (EA) for W^{3+} by the relativistic *R*-matrix method.[8] Nevertheless, as shown by Stenke,[10] the semi-empirical Lotz formula is not ideally suited for these studies, since it often leads to a strong underestimation of the measured cross in the energy range between the ionization threshold and the cross section maximum. Although the close coupling method and *R*-matrix method is very accurate, it is very time consuming. The CADW method provides a convenient and fast calculation of a single ionization cross section for complex atomic ions like tungsten,[17] but it cannot give any detailed information about EII.[21] In addition, it is difficult to deal with an EA cross section of some excited configuration lying close to the ionization thresholds for the CADW method.[22] Because pure ground configurations in the experimental beam are very difficult to obtain and the measurements of W^{q+} have often suffered from large unknown metastable fractions in the parent beams, their usefulness for benchmarking theory is limited.[23] Thus, the validity of the available data about EII data for W ions has not been tested sufficiently yet.

Here we report theoretical EISI cross section for W^{q+} ($q = 4, 5$) calculated by the flexible atomic code (FAC)[24] using the LLDW method. The calculated cross sections have been systematically compared with the available experimental and theoretical results.

2. Theoretical methods

The main EISI processes can be described by

$$e^- + A^{q+} \rightarrow A^{(q+1)+} + 2e^-, \tag{1}$$

$$e^- + A^{q+} \rightarrow [A^{q+}]^{**} + e^- \rightarrow A^{(q+1)+} + 2e^-, \tag{2}$$

where the double star superscript denotes an intermediate state to autoionize. The first process is one-step DI and the second process is two-step indirect EA via the intermediate state. Higher order indirect ionization processes, such as resonant excitation double autoionization (REDA)[25,26] and resonant excitation autodouble ionization (READI),[27,28] can also contribute to the total ionization cross section in certain resonant energy regions.

In the independent processes approximation, the total ionization cross section for the main EISI process is given by

$$\sigma_{\rm tot} = \sum_{\rm f} \sigma_{\rm f}^{\rm DI} + \sum_j \sigma_j^{\rm CE} B_j^{\rm a}, \tag{3}$$

where $\sigma_{\rm f}^{\rm DI}$ is the direct ionization cross section to the level f of $A^{(q+1)+}$ and $\sigma_j^{\rm CE}$ is the collisional excitation (CE) cross section to the level j of A^{q+}, which can then undergo autoionization forming $A^{(q+1)+}$ with a branching ratio (BR) of $B_j^{\rm a}$. The BR for autoionization of level j by emission of a single electron can be expressed as[29]

$$B_j^{\rm a} = \frac{\sum_k A_{jk}^{\rm a} B_k^{\rm r} + \sum_s A_{js}^{\rm r} B_s^{\rm a}}{\sum_k A_{jk}^{\rm a} + \sum_s A_{js}^{\rm r}}, \tag{4}$$

where $A_{jk}^{\rm a}$ is the autoionization rate from j to any level k of $A^{(q+1)+}$ and $A_{js}^{\rm r}$ is the radiative decay rate of A^{q+} from j to s. Some of the k levels may lie above the ionization limit for $A^{(q+1)+}$ and can further autoionize to form $A^{(q+2)+}$, resulting in a net single ionization event. The factor $B_k^{\rm r}$ is the radiative branching ratio accounting for the fraction of those k levels in $A^{(q+1)+}$ which radiatively relax and eventually result in a net single ionization without further autoionization to form $A^{(q+2)+}$. Similarly, some of the s levels may still lie above the ionization limit for A^{q+} but can still radiatively relax to a bound state of A^{q+}, resulting in no net ionization. The term $B_s^{\rm a}$ accounts for the fraction of those s levels in A^{q+} which autoionize by the emission of a single electron, resulting in a net single ionization event. All of the branching ratios in Eq. (4) must be solved recursively.

The formula of CE cross section $\sigma_j^{\rm CE}$ from the initial state ψ_i to the final state ψ_j can be expressed as[24]

$$\sigma_j^{\rm CE} = \frac{\pi}{k_i^2 g_i} \Omega_{ij}, \tag{5}$$

where k_i and g_i are the kinetic momentum of the incident electron and the statistical weight of the initial state, respectively. Using the factorization formula of Bar–Shalom,[30] the collision strength Ω_{ij} can be written as

$$\begin{aligned}\Omega_{ij} &= 2 \sum_k \sum_{\alpha_i \alpha_j \beta_i \beta_j} Q^k(\alpha_i \alpha_j; \beta_i \beta_j) \langle \psi_i \| Z^k(\alpha_i, \alpha_j) \| \psi_j \rangle \\ &\quad \times \langle \psi_i \| Z^k(\beta_i, \beta_j) \| \psi_j \rangle,\end{aligned} \tag{6}$$

where

$$Q^k(\alpha_i \alpha_j; \beta_i \beta_j) = \sum_{k_i k_j} [k]^{-1} P^k(\kappa_i \kappa_j; \alpha_i \alpha_j) P^k(\kappa_i \kappa_j; \beta_i \beta_j), \tag{7}$$

and

$$\begin{aligned}P^k(\kappa_i \kappa_j; \alpha_i \alpha_j) &= X^k(\alpha_i \kappa_i; \alpha_j \kappa_j) + \sum_t (-1)^{k+t} [k] \\ &\quad \times \begin{Bmatrix} j_{\alpha_i} & j_j & t \\ j_i & j_{\alpha_j} & t \end{Bmatrix} X^k(\alpha_i \kappa_i; \kappa_j \alpha_j),\end{aligned} \tag{8}$$

where $Z_M^L(\alpha_i, \alpha_j)$ and $Z_M^L(\beta_i, \beta_j)$ denote the tensors operator and X^k are two-electron radial Slater integrals.

The formula for the distorted-wave (DW) DI cross section can be expressed as[24]

$$\sigma_{\rm f}^{\rm DI}(\varepsilon_0, \varepsilon) = \frac{1}{k_i^2 g_{\rm i}} \Omega_{\rm if}, \tag{9}$$

where ε_0 and ε are the energy of the incident and the ejected electron. The collision strength $\Omega_{\rm if}$

$$\Omega_{\rm if} = 2 \sum_{k, J_{\rm T} \kappa, \alpha_{\rm i} \beta_{\rm i}} Q^k(\alpha_{\rm i} \kappa; \beta_{\rm i} \kappa) \langle \psi_i \| Z^k(\alpha_{\rm i}, \kappa) \| \Psi_{\rm f} \rangle$$

$$\times \langle \psi_i \| Z^k(\beta_i, \kappa) \| \Psi_f \rangle, \quad (10)$$

where $\Psi_f = | \psi_f, \kappa; J_T \rangle$, κ is the relativistic angular quantum number of the ejected electron, and J_T is the total angular momentum of the final state coupled with the ejected electron. The radial part Q^k is identical to that for excitation, except that one of the bound orbitals in the final state is now replaced by a free orbital.

Cross sections and decay rates were calculated using the FAC with the LLDW approximation. For a partial wave expansion to the continuum states, we set the maximum total orbital angular momentum $l_{max} = 36$ in the DW calculation, and for the higher partial wave contribution the Coulomb–Bethe approximation calculation is used to top-up the DW calculation. The potential used for the cross section is the post form of the scattering amplitude where all incident, scattered, bound, and ejected electrons see a V^N potential, where N is the total number of bound electrons in the initial target ion.[31]

3. Results and discussion

In Table 1, the ionization thresholds of the outer subshell electron are listed for the selected tungsten ions. Also some available theoretical results and NIST recommended values are tabulated for comparison. For the outermost subshell electron, namely, 5d electron for W^{q+} ($q = 4$–5), a good agreement can be found among the different calculations and NIST values. Especially for the lower charged W^{q+} ($q = 4$–5) ions, the difference between the theoretical calculations and NIST values is even less than 1.5 eV. For other 4f, 5p, and 5s electrons, our calculated ionization energies agree very well with Stenke's results[10] calculated by the MCDF code of Grant *et al.*,[33] and the difference is less than 2 eV. But a rather large discrepancy of about 8 eV for 5p electron can be noticeable between the present calculation and the CADW results.[19]

Table 1. Threshold energies (eV) for the ionization of electrons in the outer subshells of tungsten ions.

Ions	Configuration	Method	5d	4f	5p	5s
W^{4+}	$4f^{14}5d^2$	FAC	50.20	82.57	86.96	133.00
		MCDF[10]	50.28	84.41	87.27	133.3
		CADW[19]	50.03	87.25	94.82	135.91
		NIST[32]	51.6±0.3			
W^{5+}	$4f^{14}5d$	FAC	63.62	98.46	101.76	149.10
		MCDF[10]	63.58	100.3	102.2	149.4
		CADW[19]	63.98	103.62	109.58	151.44
		NIST[32]	64.77±0.4			

3.1. W^{4+}

DI channels considered of ground state configuration for W^{4+} can be expressed as

$$\begin{aligned} &e^- + [Kr]4d^{10}5s^25p^64f^{14}5d^2 \\ &\rightarrow [Kr]4d^{10}5s^2 \left\{ \begin{array}{l} 5p^64f^{14}5d \\ 5p^64f^{13}5d^2 \\ 5p^54f^{14}5d^2 \end{array} \right\} + 2e^-. \end{aligned} \quad (11)$$

The first step in the 4f EA process can be expressed as

$$\begin{aligned} &e^- + [Kr]4d^{10}5s^25p^64f^{14}5d^2 \\ &\rightarrow [Kr]4d^{10}5s^25p^6 \left\{ \begin{array}{l} 4f^{13}5d^25f \\ 4f^{13}5d^25g \\ 4f^{13}5d^2nl' \end{array} \right\} + e^-, \end{aligned} \quad (12)$$

where $6 \le n \le 10$ and $l' \le 5$. The excitation autoionization for 4f to a higher nl' subshell can be negligible. These excitation channels can undergo autoionization (AI) or radiative decay (RD) via

$$AI \rightarrow [Kr]4d^{10}5s^25p^6 \left\{ \begin{array}{l} 4f^{14}5d \\ 4f^{13}5d^2 \\ 4f^{14}nl' \end{array} \right\} + 2e^-, \quad (13)$$

$$RD \rightarrow [Kr]4d^{10}5s^25p^6 \left\{ \begin{array}{l} 4f^{14}5d^2 \\ 4f^{14}5d5[f,g]^1 \\ 4f^{13}5d^3 \\ 4f^{14}5dnl' \end{array} \right\} + h\nu + e^-. \quad (14)$$

The 5[s, p] EA channel via $5[s,p] \rightarrow nl'$ ($n \ge 5$) excitations begins with

$$\begin{aligned} &e^- + [Kr]4d^{10}5s^25p^64f^{14}5d^2 \\ &\rightarrow [Kr]4d^{10}4f^{14} \left\{ \begin{array}{l} 5[s,p]^75d^3 \\ 5[s,p]^75d^25f^1 \\ 5[s,p]^75d^25g^1 \\ 5[s,p]^75d^2nl' \end{array} \right\} + e^-, \end{aligned} \quad (15)$$

where $6 \le n \le 8$ and $l' \le 5$. These excitation channels can undergo autoionization or radiative decay via

$$AI \rightarrow [Kr]4d^{10} \left\{ \begin{array}{l} 5s^25p^64f^{14}5[d,f,g]^1 \\ 5s^25p^64f^{13}5d^2 \\ 5s^25p^54f^{14}5d^2 \\ 5s^25p^64f^{13}5d5f \\ 5s^25p^54f^{14}5d5f \\ 5s^25p^55d5[f,g]^1 \\ 5s^25p^64f^{14}nl' \\ 5s^25p^64f^{13}5dnl' \\ 5s^25p^54f^{14}5dnl' \\ 5s5p^64f^{14}5d^2 \end{array} \right\} + 2e^-, \quad (16)$$

$$RD \rightarrow [Kr]4d^{10} \left\{ \begin{array}{l} 5s^25p^64f^{14}5d^2 \\ 5s^25p^64f^{14}5d5[f,g]^1 \\ 5s^25p^64f^{13}5d^3 \\ 5s^25p^64f^{13}5d^25[f,g]^1 \\ 5[s,p]^74f^{14}5d^3 \\ 5[s,p]^74f^{14}5d^25[f,g]^1 \\ 5s^25p^64f^{14}5dnl' \\ 5s^25p^64f^{13}5d^2nl' \\ 5s^25p^54f^{14}5d^2nl' \end{array} \right\} + h\nu + e^-. \quad (17)$$

In addition, the $5s^25p^64f^{13}5d5f$, $5s^25p^54f^{14}5d5f$, $5s^25p^64f^{13}5dnl'$, $5s^25p^54f^{14}5dnl'$, and $5s5p^64f^{14}5d^2$ levels lie above the ionization threshold of W^{5+} and can further autoionize to form W^{6+}. The AI and RD channels for these

levels are given by

$$\mathrm{AI} \rightarrow [\mathrm{Kr}]4\mathrm{d}^{10} \left\{ \begin{array}{l} 5\mathrm{s}^2 5\mathrm{p}^6 4\mathrm{f}^{14} \\ 5\mathrm{s}^2 5\mathrm{p}^6 4\mathrm{f}^{13} 5\mathrm{d} \\ 5\mathrm{s}^2 5\mathrm{p}^5 4\mathrm{f}^{14} 5\mathrm{d} \end{array} \right\} + 2\mathrm{e}^-, \quad (18)$$

$$\mathrm{RD} \rightarrow [\mathrm{Kr}]4\mathrm{d}^{10}4\mathrm{f}^{14} \left\{ \begin{array}{l} 5\mathrm{s}^2 5\mathrm{p}^6 4\mathrm{f}^{14} 5\mathrm{d} \\ 5\mathrm{s}^2 5\mathrm{p}^6 4\mathrm{f}^{14} 5\mathrm{f} \\ 5\mathrm{s}^2 5\mathrm{p}^6 4\mathrm{f}^{13} 5\mathrm{d}^2 \\ 5\mathrm{s}^2 5\mathrm{p}^6 4\mathrm{f}^{13} 5\mathrm{d}5\mathrm{f} \\ 5\mathrm{s}^2 5\mathrm{p}^5 4\mathrm{f}^{14} 5\mathrm{d}^2 \\ 5\mathrm{s}^2 5\mathrm{p}^5 4\mathrm{f}^{14} nl' \\ 5\mathrm{s}^2 5\mathrm{p}^5 4\mathrm{f}^{13} 5\mathrm{d}nl' \end{array} \right\} + h\nu + \mathrm{e}^-. \quad (19)$$

All the levels of the 5d, 4f, and 5p–hole system in DI lie below the double ionization limit. DI of a 5s electron was not included because the cross section is relatively very small and as well the 5s–hole system almost 100% autoionizes resulting in a net double ionization. Figure 1 shows our resulting DI cross sections of W^{4+}. The 4f and 5p DI cross section can be comparable to that of 5d. The 4f DI cross section is even larger than the 5d DI cross section above 200 eV. Pindzola *et al.* also included the DI cross section contributions by 5d, 4f, and 5p subshells,[17] but Loch *et al.* did not include the 4f DI in Ref. [18] and the CFADC database.[19] From the present calculation, the contribution of 4f subshell should not be ignored.

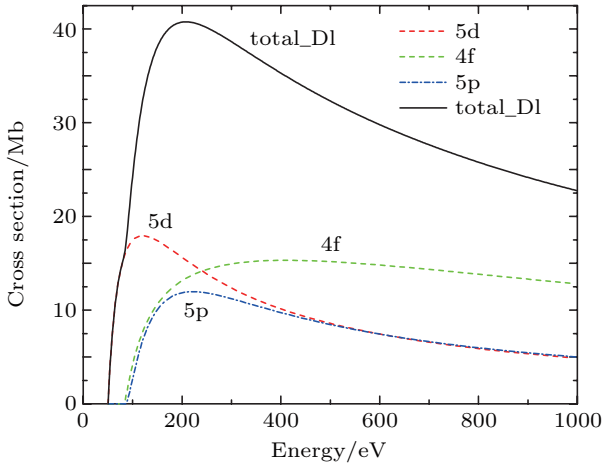


Fig. 1. (color online) DI cross sections for ground state W^{4+}. Solid line: total DI cross section, red dashed line: 5d DI, green dashed line: 4f DI, and blue dash-dotted line: 5p DI.

Table 2 lists the energies for excitations from some W^{4+} configurations, and some available results from MCDF calculation[11] and the configuration average excited energies[17] are also listed for comparison. The calculated ionization threshold for the $4f^{14}5d^2$ ground state configuration is 50.20 eV by FAC, 50.28 eV by MCDF,[11] 50.03 eV by CADW,[17] and the NIST recommended value is 51.6 ± 0.3 eV as listed in Table 1. They agree very well between each other. Our calculated energy range of excitation also agrees with that calculated by MCDF within 3 eV. The lowest autoionizing levels belong to the $4f \rightarrow 6s$ and the $5p \rightarrow 5d$ excitations from Stenke's calcualtion.[11] Our calculation suggests that all levels of $4f \rightarrow 6s$ are below the autoionization threshold. In the case of $4f \rightarrow 6p$, $5p \rightarrow 5d$, $5p \rightarrow 6s$, and $5p \rightarrow 6p$ excitations, their levels straddle the ionization threshold. For the $5p \rightarrow 5d$ excitation, our calculation reveals that 9 levels of the initial $5s^2 5p^6 4f^{14} 5d^2$ configuration are spread over 6.0 eV, and 110 levels of the final $5s^2 5p^6 4f^{14} 5d^2$ configuration are spread over 24.2 eV, which is close to the MCDF calculation of 28.8 eV as listed in Table 2. The levels of the initial and final configuration are respectively spread over 6.4 eV and 22.0 eV in Pindzola's calculation.[17] With respect to the lowest level of the ground configuration, 26 of the 110 levels are autoionizing in Pindzola's calculation;[17] however, 37 of the 110 levels are autoionizing in our calculation. Because the $5p \rightarrow 5d$ excitation has the largest relative strength in all the inner-shell excitations as shown in Fig. 2(b), the different consideration of the possible EA levels will cause a very different result, as shown below.

Table 2. Energies for excitations from some W^{4+} configurations.

Configuration	Transition	FAC	MCDF[10]	CADW[17]
$4f^{14}5d^2$	$4f \rightarrow 5d$	30.37–41.12	32.06–42.95	35.03
	$4f \rightarrow 5f$	59.06–72.35		64.47
	$4f \rightarrow 5g$	68.79–78.33		73.40
	$4f \rightarrow 6s$	37.55–47.39	40.44–50.52	42.94
	$4f \rightarrow 6p$	45.17–57.47		51.78
	$4f \rightarrow 6d$	57.55–68.26		62.85
	$4f \rightarrow 6f$	68.0–79.20		72.89
	$4f \rightarrow 6g$	73.41–82.89		77.65
	$4f \rightarrow 7s$	59.21–68.65	61.33–71.14	
	$5p \rightarrow 5d$	36.10–60.29	36.45–61.25	43.95
	$5p \rightarrow 5f$	63.71–78.33		72.11
	$5p \rightarrow 6s$	42.22–64.88	43.56–66.97	50.91
	$5p \rightarrow 6p$	49.83–74.97		59.68
	$5p \rightarrow 6d$	62.28–85.79		70.65
	$5p \rightarrow 6f$	72.56–94.78		80.52
	$5p \rightarrow 7s$	63.73–85.15	64.30–86.80	
	$5s \rightarrow 6s$	88.11–97.22		92.01
	$5s \rightarrow 6p$	95.85–106.32		100.69
	$5s \rightarrow 6d$	108.3–117.3		111.66

In Fig. 2(a), the calculated EA cross section from the 4f subshell is shown. The largest contribution comes from the $4f \rightarrow 5l'$ and $4f \rightarrow 6l'$ EA. The contribution from $4f \rightarrow 7l'$, $4f \rightarrow 8l'$, and $4f \rightarrow 9l'$ also cannot be negligible. The contribution of 4f EA to the total EA cross section is about 23% at 83.2 eV, but it was not included in the CFADS database.[19] In Fig. 2(b), we ploted the $5[\mathrm{s,p}] \rightarrow nl'$ EA cross section as a function of electron energy, along with the total 4f EA cross section for comparison. The largest contribution comes from $5[\mathrm{s,p}] \rightarrow 5l'$ EA. The contribution of $5[\mathrm{s,p}] \rightarrow 7l', 8l'$ is less than 10% at peak EA position.

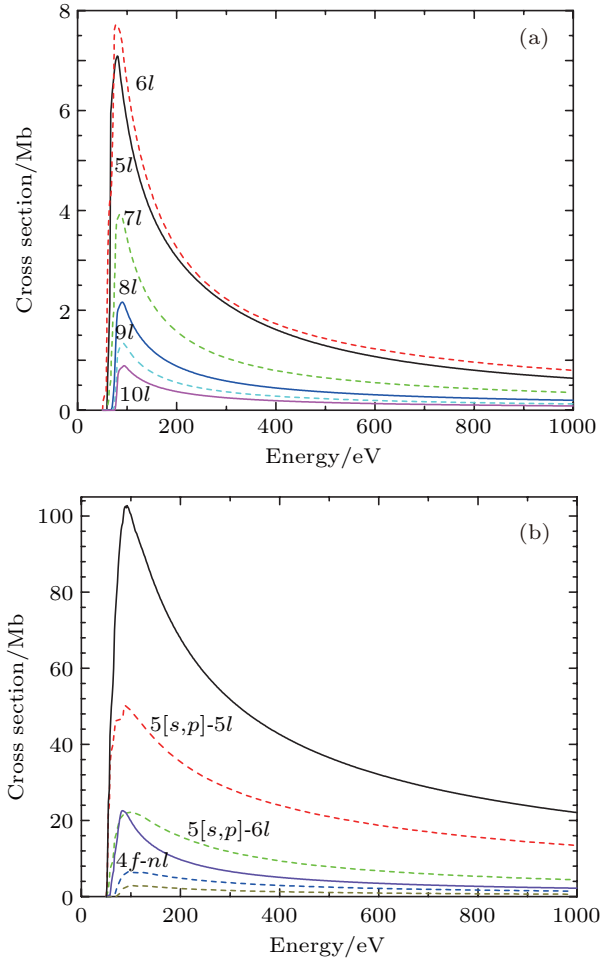


Fig. 2. (color online) Our calculated EA cross sections for ground state W^{4+}. (a) $4f \rightarrow nl'$ EA. Solid black line: $4f \rightarrow 5d, 5f, 5g$ EA, red dashed line: $4f \rightarrow 6l'$ EA, green dashed line: $4f \rightarrow 7l'$ EA, blue solid line: $4f \rightarrow 8l'$ EA, cyan dashed line: $4f \rightarrow 9l'$ EA, and magenta dashed line: $4f \rightarrow 10l'$ EA. (b) EA cross sections for ground state W^{4+}. Solid line: total EA cross section included $4f \rightarrow nl'$ EA contribution, red dashed line: $5[s,p] \rightarrow 5d, 5f, 5g$ EA, green dashed lines: $5[s,p] \rightarrow 6l'$ EA, blue dashed lines: $5[s,p] \rightarrow 7l'$ EA, and dark yellow dashed lines: $5[s,p] \rightarrow 8l'$ EA. The results of $4f \rightarrow nl'$ EA are also plotted for comparison using the voilet line.

Figure 3 shows a comparison of our calculated results with the available theoretical and experimental results for the EISI of the ground state W^{4+}. For the case of the DI cross section, the same contributions of 5d, 4f, and 5p subshells were considered into the present and Pindzola's calculation. As shown in Fig. 3, the present LLDW DI cross section is lower than that of the CADW. The difference is about 10%. In the calculation of EA cross section, Pindzola *et al.* included the contributions of $5p \rightarrow 5d$, $5s \rightarrow 5d, 6s, 6p, 6d$, and $4f \rightarrow 5f, 5g, 6l$ ($l = s, p, d, f, g$) EA. For the case of $5p \rightarrow 5d$ excitation, they only included 21% of the excitation cross section at the average threshold, due to that 26 of the 110 levels in the final configuration are autoionizing as mentioned above. In our calculation shown as the black solid line in Fig. 3, we also included the same EA contribution as the inclusion of Pindzola's calculation except for $5p \rightarrow 5d$ EA, for which we only included the contribution from the highest 21 levels of 37 autoionization levels. Our calculated total EISI cross section in this situation is very close to Pindzola's result and the experiment;[11] however, our theoretical total cross section considering all contributions is larger than the measured cross section by about 41% at 125.7 eV.

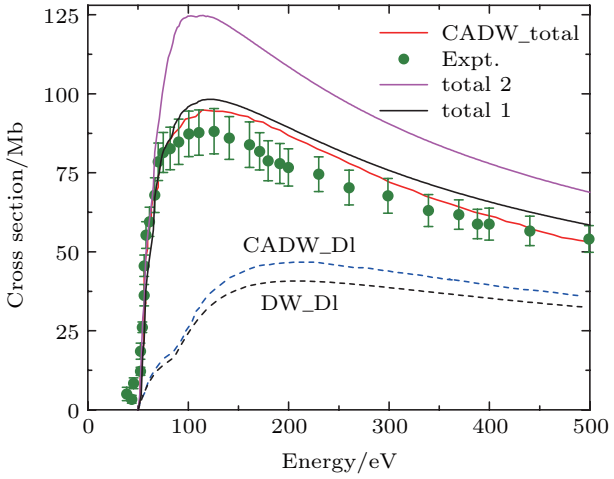


Fig. 3. (color online) Total DI cross section and the total EISI cross sections for ground state W^{4+}. Black dashed line: the present LLDW total DI cross section, blue dashed line: CADW total DI cross section,[17] black solid line: our calcualted total cross section in which the same EA contribution were considered, red solid line: Pindzola's calculated result,[17] and magenta solid line: our calculated total cross section with inclusion of all EA contributions. The experimental results of Stenke *et al.*[11] are plotted using solid circles.

3.2. W^{5+}

DI channels considered of ground state configuration for W^{5+} can be expressed as

$$\begin{aligned} &e^- + [Kr]4d^{10}5s^25p^64f^{14}5d \\ &\rightarrow [Kr]4d^{10}\left\{\begin{array}{l} 5s^25p^64f^{14} \\ 5s^25p^64f^{13}5d \\ 5s^25p^54f^{14}5d \\ 5s5p^64f^{14}5d \end{array}\right\} + 2e^-. \end{aligned} \tag{20}$$

The first step in the 4f EA process can be expressed as

$$\begin{aligned} &e^- + [Kr]4d^{10}5s^25p^64f^{14}5d \\ &\rightarrow [Kr]4d^{10}5s^25p^6\left\{\begin{array}{l} 4f^{13}5d5[f,g]^1 \\ 4f^{13}5dnl' \end{array}\right\} + e^-, \end{aligned} \tag{21}$$

where $6 \le n \le 10$ and $l' \le 5$. The excitation autoionization for 4f to a higher nl' subshell can be negligible. These excitation channels can undergo AI or RD via

$$AI \rightarrow [Kr]4d^{10}5s^25p^6 + 2e^-, \tag{22}$$

$$RD \rightarrow [Kr]4d^{10}5s^25p^6\left\{\begin{array}{l} 4f^{14}5d \\ 4f^{14}5d5[f,g]^1 \\ 4f^{13}5d^2 \\ 4f^{14}nl' \end{array}\right\} + h\nu + e^-. \tag{23}$$

The 5[s, p] EA channel via $5[s,p] \rightarrow nl'$ ($n \ge 5$) excitations begins with

$$e^- + [Kr]4d^{10}5s^25p^64f^{14}5d$$

$$\rightarrow [\mathrm{Kr}]4\mathrm{d}^{10}4\mathrm{f}^{14}\left\{\begin{array}{l}5\mathrm{s}5\mathrm{p}^5 5\mathrm{d}^2\\ 5[\mathrm{s},\mathrm{p}]^7 5\mathrm{d}5[\mathrm{f},\mathrm{g}]^1\\ 5[\mathrm{s},\mathrm{p}]^7 5\mathrm{d}nl'\end{array}\right\}+\mathrm{e}^-, \quad (24)$$

where $6 \le n \le 10$ and $l' \le 5$. These excitation channels can undergo autoionization or radiative decay via

$$\mathrm{AI} \rightarrow [\mathrm{Kr}]4\mathrm{d}^{10}5\mathrm{s}^2\left\{\begin{array}{l}5\mathrm{p}^6 4\mathrm{f}^{14}\\ 5\mathrm{p}^6 4\mathrm{f}^{13}5\mathrm{d}\\ 5\mathrm{p}^5 4\mathrm{f}^{14}5\mathrm{d}\\ 5\mathrm{p}^6 4\mathrm{f}^{13}nl'\\ 5\mathrm{p}^5 4\mathrm{f}^{14}nl'\end{array}\right\}+2\mathrm{e}^-, \quad (25)$$

$$\mathrm{RD} \rightarrow [\mathrm{Kr}]4\mathrm{d}^{10}\left\{\begin{array}{l}5\mathrm{s}^2 5\mathrm{p}^6 4\mathrm{f}^{14}5\mathrm{d}\\ 5\mathrm{s}^2 5\mathrm{p}^6 4\mathrm{f}^{14}5[\mathrm{f},\mathrm{g}]^1\\ 5\mathrm{s}^2 5\mathrm{p}^6 4\mathrm{f}^{13}5\mathrm{d}^2\\ 5\mathrm{s}^2 5\mathrm{p}^6 4\mathrm{f}^{13}5\mathrm{d}5[\mathrm{f},\mathrm{g}]^1\\ 5[\mathrm{s},\mathrm{p}]^7 4\mathrm{f}^{14}5\mathrm{d}^2\\ 5[\mathrm{s},\mathrm{p}]^7 4\mathrm{f}^{14}5\mathrm{d}5[\mathrm{f},\mathrm{g}]^1\\ 5\mathrm{s}^2 5\mathrm{p}^6 4\mathrm{f}^{14}nl'\\ 5\mathrm{s}^2 5\mathrm{p}^6 4\mathrm{f}^{13}5\mathrm{d}nl'\\ 5\mathrm{s}^2 5\mathrm{p}^5 4\mathrm{f}^{14}5\mathrm{d}nl'\end{array}\right\}+h\nu+\mathrm{e}^-. \quad (26)$$

Table 3. Energies for excitations from some W^{5+} configurations.

Configuration	Transition	FAC	MCDF[10]	CADW[17]
$4f^{14}5d$	$4f \rightarrow 5d$	32.29–42.0	34.13–100.0	37.22
	$4f \rightarrow 5f$	65.01–76.50		71.32
	$4f \rightarrow 5g$	79.01–84.55		83.66
	$4f \rightarrow 6s$	42.55–48.71		48.16
	$4f \rightarrow 6p$	51.02–60.03		58.11
	$4f \rightarrow 6d$	65.23–73.31		71.03
	$4f \rightarrow 6f$	77.83–85.57		83.25
	$4f \rightarrow 6g$	85.13–90.57		89.79
	$5p \rightarrow 5d$	36.57–58.50	36.99–59.38	44.79
	$5p \rightarrow 5f$	68.95–90.30		77.47
	$5p \rightarrow 6s$	46.46–66.78		54.64
	$5p \rightarrow 6p$	54.88–77.85		64.50
	$5p \rightarrow 6d$	69.15–90.22		77.30
	$5p \rightarrow 6f$	81.55–101.97		89.32
	$5s \rightarrow 5d$	82.66–90.49		85.88
	$5s \rightarrow 6s$	93.40–97.48		96.49
	$5s \rightarrow 6p$	101.97–108.92		106.25
	$5s \rightarrow 6d$	116.22–121.67		119.05

All the levels of $5l$ and 4f–hole system in DI lie below the double ionization limit. Figure 4(a) plotted the DI cross section as the electron energy. It can be seen that the major contributions to the DI cross section come from the 4f subshell. Comparing with the above tungsten ions, the contribution of 5d DI for the ground state W^{5+} reduces and even is smaller that of the 5p subshell. The 5s DI begins to contribution to the EISI of W^{5+}, although its cross section is small. Although Pindzola *et al.* included the DI crosss section contributions by 5d, 4f, 5p, and 5s subshells,[17] Loch *et al.* did not include the 4f DI in Ref. [18] and the CFADC database.[19] The contributions of various EA to the EISI cross section are shown in Fig. 4(b). The largest contribution comes from $5p \rightarrow nl'$ EA.

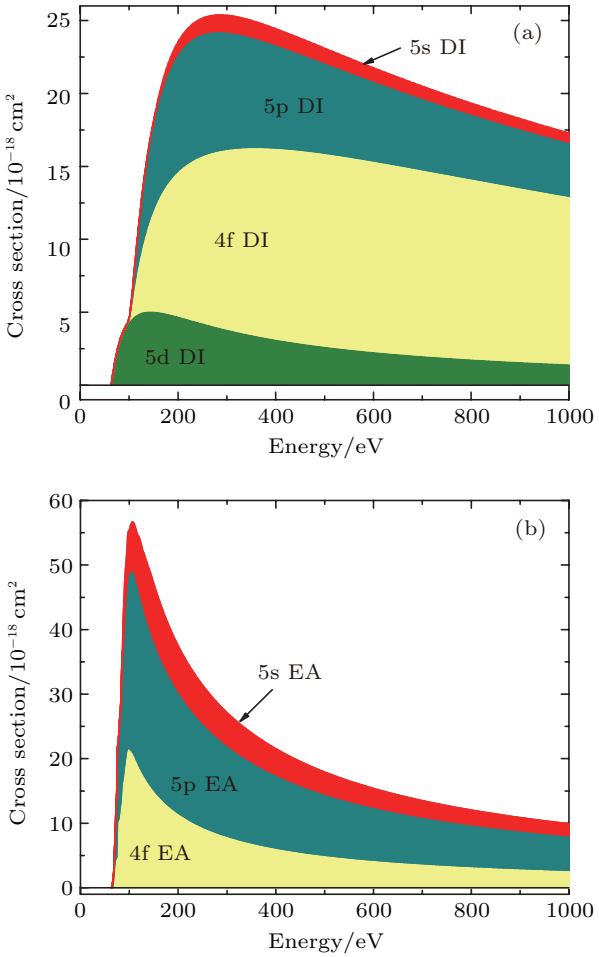


Fig. 4. (color online) Our calculated (a) DI and (b) EA cross sections for ground state W^{5+}.

Figure 5 shows a comparison of our calculated results with available theoretical and experimental results for the EISI of the ground state W^{5+}. Similar to the case of ground state W^{4+}, the present LLDW DI cross section is lower than that of the CADW, althouth the same contribution of 5d, 4f, 5p, and 5s subshells were considered in the present and Pindzola's calculations. The maximum difference is about 13%. In the calculation of EA cross section, Pindzola *et al.* included the contributions of $5p \rightarrow 5f, 6p, 6d, 6f$, $5s \rightarrow 5d, 6s, 6p, 6d$, and $4f \rightarrow 5f, 5g, 6l$ $(l = s, p, d, f, g)$ EA. In our calculation shown as the black solid line in Fig. 5, we also included the same EA contribution as the inclusion of Pindzola's calculation. Similar to Fig. 3, our calculated total EISI cross section of the ground state W^{5+} in such a situation is very close to Pindzola's result and the experiment;[11] however, our theoretical total cross section considering all contributions is still larger than the measured cross section by about 15% at 146.1 eV.

Figure 6 shows the theoretical EISI cross section from the ionization threshold to 1000 eV, along with the recent experimental results.[13] Our calculated EISI cross section of W^{5+} reasonably agrees with the experiment at the high energy region. The difference between the calculation and experiment

at near threshold may partly contribute to the ionization of metastable ions in the incident ion beam.

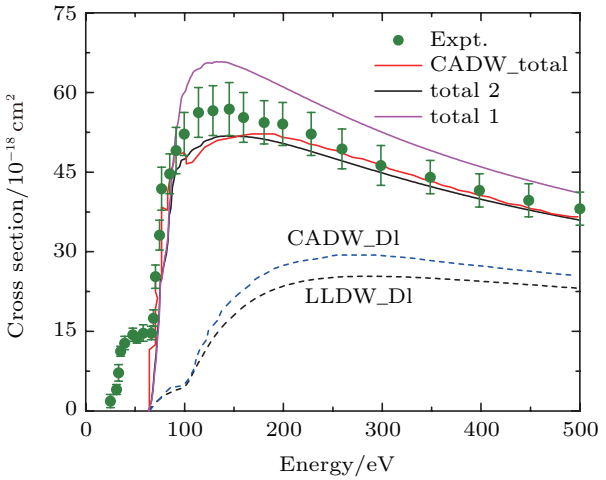


Fig. 5. (color online) Total DI cross section and the total EISI cross sections for ground state W^{5+}. Black dashed line: the present LLDW total DI cross section, blue dashed line: CADW total DI cross section,[17] black solid line: our calculated total cross section with inclusion of the same EA contribution as in the CADW calculation, red solid line: Pindzola's calculated result,[17] and magenta solid line: our calculated total cross section with inclusion of all EA contributions. The experimental results of Stenke *et al.*[11] are plotted using solid circles.

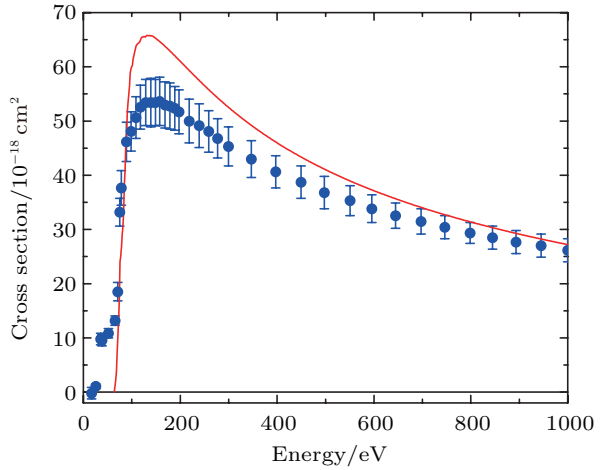


Fig. 6. (color online) A comparison of our total EISI cross section (red line) for ground state W^{5+} with Spruck's experiment[13] (blue circles).

4. Conclusion

We have calculated the EISI cross section of ground state configuration W^{q+} ($q = 4$–5) using the FAC code in the LLDW method. A systematic comparison with the available theoretical and experimental results has been performed. Our calculated DI cross section is smaller than the CADW results. Although several available theoretical total cross sections agree reasonably well with the cross beam experiment, the contributions from some significant channels were not included in those calculations. In the case of considering the same channel contributions, our results also agree with the measured cross sections; however, our calculated total DI+EA cross sections with inclusion of all channels contribution are larger than the experiment, especially at peak position. The difference between the present DW calculation and the experiment deceases with the increasing of the charged state for tungsten ions.

Acknowledgment

The authors would like to thank Dr. Duck-Hee Kwon for her good suggestion and helpful discussion.

References

[1] Bolt H, Barabash V, Krauss W, Linke J, Neu R, Suzuki S and Yoshida N: ASDEX Upgrade Team 2004 *J. Nucl. Mater.* **329-333** 66
[2] Hinnov E 1974 *J. Nucl. Mater.* **53** 9
[3] Isler R C, Neidigh R V and Cowan R D 1977 *Phys. Rev. A* **63** 295
[4] Dux R, Janzer A and Pütterich T: ASDEX Upgrade Team 2011 *Nucl. Fusion* **51** 053002
[5] Reader J 2009 *Phys. Scr.* **T134** 014023
[6] Pitts R A, Carpentier S, Escourbiac F, Hirai T, Komarov V, Kukushkin A S, Lisgo S, Loarte A, Merola M, Mitteau R, Raffray A R, Shimada M and Stangebyb P C 2011 *J. Nucl. Mater.* **415** S957
[7] Skinner C H 2009 *Phys. Scr.* **T134** 014022
[8] Ballance C P, Loch S D, Pindzola M S and Griffin D C 2013 *J. Phys. B-At. Mol. Opt.* **46** 055202
[9] Montague R G and Harrison M F A 1984 *J. Phys. B-At. Mol. Opt.* **17** 2707
[10] Stenke M, Aichele K, Harthiramani D, Hofmann G, Steidl M, Völpel R and Salzborn E 1995 *J. Phys. B-At. Mol. Opt.* **28** 2711
[11] Stenke M, Aichele K, Harthiramani D, Hofmann G, Steidl M,Völpel R, Shevelko V P, Tawara H and Salzborn E 1995 *J. Phys. B-At. Mol. Opt.* **28** 4853
[12] Rausch J, Becher A, Spruck K, Hellhund J, Borovik Jr A, Huber K, Schippers S and Müller A 2011 *J. Phys. B-At. Mol. Opt.* **44** 165202
[13] Spruck K, Becker A, Borovik Jr A, Gharaiheh M F, Rausch J, Schippers S and Müller A 2014 *J. Phys. -Conf. Ser.* **488** 062026
[14] Kwon D H, Rhee Y J and Kim Y K 2006 *Int. J. Mass Spectrom.* **252** 213
[15] Jonauskas V, Kučas and Karazija R 2009 *Lith. J. Phys.* **49** 415
[16] Pindzola M S and Griffin D C 1992 *Phys. Rev. A* **46** 2486
[17] Pindzola M S and Griffin D C 1997 *Phys. Rev. A* **56** 1654
[18] Loch S D, Ludlow J A, Pindzola M S, Whiteford A D and Griffin D C 2005 *Phys. Rev. A* **72** 052716
[19] http://www-cfadc.phy.ornl.gov
[20] Vainshtein L, Beigman I, Mertens Ph, Brezinsek S, Pospieszczyk A and Borodin D 2011 *J. Phys. B-At. Mol. Opt.* **44** 125201
[21] Borovik A, Brandau C, Jacobi J, Schipper S and Müller A 2011 *J. Phys. B-At. Mol. Opt.* **44** 205205
[22] Loch D S, Pindzola, Ballance P C, Griffin D C, Mitnik D M, Badnell N R, O'Mullane M G, Summers H P and Whiteford A D 2002 *Phys. Rev. A* **66** 052708
[23] Dere P K 2007 *Astron. Astrophys.* **466** 771
[24] Gu M F 2008 *Can. J. Phys.* **86** 675
[25] Nakamura N, Tobiyama H, Nohara H, Kato D, Watanabe H, Currell F J and Ohtani S 2006 *Phys. Rev. A* **73** 020705(R)
[26] Badnell N R and Pindzola M S 1993 *Phys. Rev. A* **47** 2937
[27] Henry R J W and Msezane A Z 1982 *Phys. Rev. A* **26** 2545
[28] Müller A, Hofmann G, Tinschert K and Salzborn E 1988 *Phys. Rev. Lett.* **61** 1352
[29] Kwon D H and Savin D W 2012 *Phys. Rev. A* **86** 022701
[30] Bar-shalom A, Klapisch M and Oreg J 1988 *Phys. Rev. A* **38** 1773
[31] Pindzola M S, Griffin D C and Macek J H 1995 *Phys. Rev. A* **51** 2186
[32] Kramida A and Shirai T 2009 *At. Data Nucl. Data Tables* **95** 305
[33] Grant I P, McKenzie B J, Norrington P H, Mayers D F and Pyper N C 1980 *Comput. Phys. Commun.* **21** 207
[34] Hahn M, Bernhardt D, Grieser M, Krantz C, Lestinsky M, Müller A, Novotný O, Repnow R, Schippers S, Wolf A and Savin D W 2011 *Astrophys. J.* **729** 76